

IN SILICO ANALYSIS OF THE KEY ENZYMES INVOLVED IN SYNTHESIS OF SECONDARY METABOLITES IN *CAMELLIA SINENSIS*

S. W. Maina, J. K. Kinyua and D. W. Kariuki

Collenge of Health Sciences, Jomo Kenyatta University of Agriculture and Technology, Nairobi, Kenya

E-mail: wairimusylvia@yahoo.com

Abstract

Tea is one of the most popular beverages worldwide, native to Southeast Asia but currently cultivated in over 35 countries. Studies on its chemical composition reveal that polyphenol metabolites account for 25% to 35% of the total dry weight. Tea has many health benefits owing to secondary metabolites whose level of expression in various tea clones determine tea flavor. The flavor (taste and aroma) and the color of processed tea are used to assess its quality and therefore a detailed analysis of key enzymes involved in the synthesis of secondary metabolites is necessary. This study employed a computational approach in the analysis of these enzymes to gain insight into the mechanism of synthesis of these bioactive secondary metabolites. Biological databases were used to retrieve amino acid sequences of these key enzymes. Consensus conserved regions in these sequences were identified from highly identical homologs which were useful in modeling the enzymes' three dimensional structures. A total of 14 key enzymes were analyzed and pockets and cavities in their structures; hence the putative substrate binding sites determined, which gave insight into the enzymes-substrate as well as enzyme cofactor interactions. The preferred orientations of the interactions between substrates and/or co-factors with the enzymes were also simulated through molecular docking. Analysis of these enzymes revealed unique enzyme structures and very specific substrate and co-factor preference. This analysis offers a platform for optimization of selective expression of these key enzymes through gene expression assays that can potentially alter the quality yield of tea clones.

Key words: *Camellia sinensis*, secondary metabolite, conserved regions, pockets and cavities, molecular docking

1.0 Introduction

Tea is one of the most widely consumed beverages in the world second only to water (Wang, *et al.*, 2008) as well as one of the most economically important crops. It is native to China, Japan and Southeast Asia. Tea was introduced by the British in India, Sri Lanka, and by the Dutch in Indonesia. Later, in the 20th century commercial production began in Kenya, Tanzania, and Malawi. Currently it is produced by more than 35 countries (Gesimba *et al.*, 2005). Tea seedlings were introduced to Kenya from India by G.W.L. Caine in 1903, however, commercial cultivation began in 1924.

The commercial importance of the tea plant (*Camellia sinensis*) is due to its popularity as a refreshing health drink and as a source of important secondary metabolites. The leaves of assamica and sinensis, varieties are used to manufacture tea. The flavor and colour of processed tea is used to assess quality of tea. The non-volatile constituents are responsible for taste while aroma is due to the volatile constituents. A strong attractive aroma is the most important and desirable characteristic of good quality tea. In recent years, tea has attracted more and more attention because of its reported health benefits particularly as an antioxidant and anticarcinogenic. The flavonoids of tea are generally believed to be responsible for these effects.

Over 500 flavour compounds have been identified in tea (Rawat and Gulati, 2008). Tea catechins are most widely studied. They are water-soluble compounds which impart bitterness and astringency to tea. They have been reported to have ant oxidative, ant carcinogenic, antiallergenic, anti-inflammatory, and vasodilatory properties. Catechins are synthesised by the flavonoid biosynthetic pathway starting with phenylalanine as the precursor. Almost all of the characteristics of manufactured tea, including its taste, colour and aroma, have been found to be associated directly or indirectly with catechins (Wang *et al.*, 2010).

The aroma of tea is attributed to the volatile flavour compounds (VFC) in tea. Most volatile compounds originate from large precursor molecules present in tea leaves that include products of lipid breakdown, terpenoids and

phenolics, which are present as bound glycosides in tea leaves and are released upon the action of enzymes like glucosidases (Rawat and Gulati, 2008).

Tea processing is known to enhance the release of volatile compounds from bound precursors (Ravichandran, 2002). VFCs derived from terpenoid related compounds are important components of aroma because of their desirable sweet flowery aroma. These VFCs include monoterpene alcohols like linalool and its oxides, geraniol and products of oxidation of carotenoids like β -ionone. The precursors for the synthesis of monoterpenes and tetraterpenes like carotenoids are provided by the Methylerythritol Phosphate pathway in plastids and precursors for monoterpene and carotenoid synthesis are Geranyl Pyrophosphate and Geranylgeranyl Pyrophosphate respectively.

2.0 Materials and Method

2.1 Enzyme Selection

This study was based on focusing on analysis of the secondary metabolism genes. The secondary metabolism genes, mostly discovered through EST sequencing were obtained from NCBI. The sequences of enzymes responsible for their synthesis were obtained from protein database <http://www.uniprot.org/help/uniprotkb>). The key enzymes for the study were identified according to Park *et al.*, 2004. The enzymes studied were PAL, C4H, 4CL, CHS, CHI, F3H, F-3,5-H, DFR, FLS, ANS, ANR and ANR2, BPR, LAR and PSY.

2.2 Identification of Consensus Conserved Region

To determine the conserved regions in the enzymes, the products were subjected to BLASTp analysis using Protein Databank to get closely related sequences from other species which have known structures. The highly identical homologs sequences were obtained and aligned using clustalW according to Larkin *et al.*, 2007 to identify the consensus conserved region of each of the enzymes.

2.3 Domain Analysis and Protein Modeling

The 3 dimensional structure of the enzyme structures were modeled using the PHYRE2 according to Kelly and Sternberg 2009 server available at (www.sbg.bio.ic.ac.uk/phyre2/). The submitted protein sequences were first scanned against a large sequence database using PSI-BLAST. The profile generated by PSI-BLAST was then processed by the neural network secondary structure prediction program Pspred and the protein disorder Disopred. The predicted presence of alpha helices, beta strands and disordered regions was represented graphically together with color coded by confidence bar. This was displayed in the final model.

The amino acid sequences of a representative set of all known three-dimensional protein structures were compiled; these sequences were processed by scanning against a large protein sequence database. This resulted in a database of profiles or HMMs, one for each known 3D structure. The user sequence of interest was similarly processed to form a profile/HMM. This user profile was then scanned against the database of profiles using profile-profile or HMM-HMM alignment technique. The alignment techniques also took into account patterns of predicted or known secondary structure elements and they were scored in terms of coverage and confidence to the target sequence. The final model was built using the best 20 domains; best in terms of sequence coverage and the alignment. This was based on the fact that many proteins contain multiple protein domains. PHYRE2 provided a table of template matches color-coded by confidence and indicating the region of the user sequence matched. This aided in the determination of the final protein.

2.4 Binding Pocket Analysis

The predicted 3 Dimensional structures were used to locate the structural pockets and cavities in the proteins. 3Dligandsite server was used to determine protein binding site according to Wass *et al.*, 2009. Structures that were modeled with confidence > 90% were automatically submitted to 3Dligand site. Ligands bound to the new structures similar to the query were superimposed onto the model and were used to predict the binding sites. Structures homologous to the query that have ligands bound were searched. MAMMOTH is used to perform a full structural scan of the modeled structure against a library of protein structures with bound ligands. Upto the top 25 scoring (using MAMMOTH -lnE score) are retained for analysis. These structures are aligned with the modeled structure using TAlign. Single linkage clustering is used to group the ligands. Confirmation of the presence of the

binding sites was done by identifying pockets and cavities. This was done using CASTp server available at <http://sts.bioengr.uic.edu/castp>. CASTp measures analytically the area and volume of each pocket and cavity.

2.5 Docking

Computational simulation of a candidate ligand binding to the enzyme (receptor) was done to show the preferred orientation of both molecules when they are interacting. This interaction was aimed at predicting the association/affinity between the two molecules. The approach used in docking these ligands was shape complementarity. Docking was done using Molsoft available at (www.molsoft.com)

3.0 Results and Discussion

3.1 Protein Structure Prediction and Modeling

The 3 dimensional structure of the protein as modeled using the PHYRE2 according to Kelly and Sternberg 2009 server available at (www.sbg.bio.ic.ac.uk/phyre2/). The top 20 best hits in the alignment of each of the target enzymes sequences are used in modeling each of the enzymes to avoid computer load. The percentage confidence of the final model is determined from the templates and the percentage coverage is calculated based on the residues match between the target and the template that are used in modeling. The PSY enzyme has 4 templates that are selected to model the protein based on heuristics to maximise confidence, percentage identity and alignment coverage. It is the only low quality model less than 70% confidence. The model is modeled using ab initio approach where only 46 residues (64%) are modeled as shown in Table 1.

Table 1: Templates used in modeling various proteins using PHYRE 2 server based on PDB templates in PHYRE 2 server with the percentage confidence and coverage

Enzyme	Template and its PDB information	Confidence (%)	Coverage (%)
PAL	D1W27A, L-aspartate like fold, SUPERFAMILY: L-aspartate like, FAMILY: PAL/HAL	100	96
C4H	C2Q9FA an oxidoreductase used Chain: A of : PDB molecule: cytochrome P450 46a1	100	94
4CL	c3ni2A. a ligase, Chain: A of crystal structures of a populus tomentosa 4-2 coumarate: COA ligase was used.	100	89
CHS	C3TSYA. A ligase, transferase, Chain: A of fusion protein 4-coumarate COA ligase 1, reveratrol, PDB title: 4-coumaryl-COA ligase: stilbene synthase fusion protein was used	100	99
CHI	C4d00A an ISOMERASE, Chain:A of chalcone-flavanone isomerase family protein was used. PDB title: the crystal structure of Arabidopsis thaliana fatty-acid binding protein2 at 3g63170 (atfap1)	100	77
F3H	d1gp6A, FOLD was a double stranded beta helix, SUPERFAMILY: clavamate synthase-like, FAMILY: penicillin synthase-like	100	89
F-3,5-H	PDB template was c3ebsA. An oxidoreductase, Chain:A PDB Molecule: cytochrome p450 2a6	100	88
DFR	C2iodD an oxidoreductase , Chain: D: PDB Molecule: DIHYDROFLAVONOL 4-REDUCTASE;PDB Title: Binding of two substrate analogue molecules to 2 dihydroflavonol-4-reductase alters the functional geometry 3 of the catalytic site	100	93
FLS	d1gp6A, FOLD: is a double stranded beta helix, SUPERFAMILY: clavamate synthase-like, FAMILY: penicillin synthase-like	100	98
ANS	D1GP6A, FOLD is double stranded beta helix, SUPRERFAMILY: clavamate synthase-like, FAMILY: penicillin synthase like.	100	98
ANR	C1Z45A, an isomerase, Chain: A PDB Molecule gal10 biofunctional protein; was used.	100	92
BPR	c3ptkB. PDB header: hydrolase, Chain:B PDB Molecule: Beta-glucosidase	100	93

	os4glu12, PDB title: the crystal structure of rice (oryza sativa 1.) os4bglu12.		
LAR	C1Z7EC. The template is a hydrolase. Chain: C: PDB Molecule: protein arna; PDB Title: crystal structure of full length arna	100	90
PSY	1) d1ezfA, FOLD: Terpenoid synthase, Superfamily: terpenoid synthases, Family: squaline synthase 2) c4hd1A, PDB Header: transferase, Chain: A: PDB Molecule: Squaline synthas hpnc 3) C3p5rB, PDB header: lyase, Chain: B: PDB Molecule: taxadiene synthase 4) C2zcpA, PDB header:transferase Chain: A: PDB Molecule:dehydrosqualene synthase;	90	64

3.2 Alignment of the Domains that were used to Establish Each Enzymes Model

Table 2: aligned regions for PAL, C4H and 4CL. The tables below show the domains used to establish the enzyme model by aligning the top 20 best hits that match highly with the target sequence. The confidence key in table 6 is used to show the probability with which the target sequence matches the available structures in terms of the different colors.

Aligned regions for PAL

Aligned regions for PAL		Aligned regions for C4H		Aligned regions in 4CL	
1	d1w27a			1	c3ni2
2	c3nz4A	1	c2q9f	1	A_
3	c4babC_			2	d1pg4
4	c1t6pF	2	c2f9q	2	a_
5	d1t6ja	3	c3pm	3	d1ry2
6	d1gkma		0A	3	a_
7	c3czoD	4	c3e4e	4	c2vsq
8	c3unvB		A_	4	A_
9	c2gveA	5	d1nr6	5	c3tsy
10	c2o6yF		a_	5	A_
11	c2nynD	6	c2hi4	6	c3e7w
12	c2lmdA		A_	6	A_
13	c1kkoB	7	d1r9o	7	d3cw9
14	c4hecB		a_	7	a1
15	c1yvya	8	d1po5	8	d1md
16	d2olra1		a_	8	ba_
17	d1mija	9	d3czh	9	c2d1t
18	d1z0sa1		a1	9	A_
19	c1z0zC	1	c3na0	1	c3r44
20	d7aata		B_	0	A_
		1	c2x2n	1	c3etc
			B_	1	B_
		1	c3ebs	1	c4dg8
			A_	1	A_
		2		2	
		1	d2nnj	1	d1icl

	3	a1	3	a_
	1	c3ruk	1	c3gaw
	4	D_	4	B_
	1	d1tqn	1	c3eyn
	5	a_	5	B_
	1	c3k9v	1	d1am
	6	B_	6	ua_
	1	c3eqm	1	c4fug
	7	A_	7	D_
	1	c3jiv	1	c4dg9
	8	A_	8	A_
	1	c3hf2	1	c3rg2
	9	A_	9	H_
	2	d2ii2	2	c1amu
	0	a1	0	B_

Table 3: Aligned regions for CHS, CHI and F3H. . The tables below show the domains used to establish the enzyme model by aligning the top 20 best hits that match highly with the target sequence. The confidence key in table 6 is used to show the probability with which the target sequence matches the available structures

Aligned region for CHS		Aligned regions in CHI		Aligned region in F3H	
1	c3tsy A_	1	c4doo A_	1	d1gp6 a_
2	c1cmf A_	2	d1eyq a_	2	c3oox A_
3	c2d3m A_	3	c4dol A_	3	d1odm a_
4	c3ale B_	4	c4doi B_	4	d1w9y a1
5	d1bi5 a1	5	c4dok A_	5	d1dcs a_
6	c3v7l A_	6	c2yue A_	6	c3on7 C_
7	c3oit B_	7	d1o9y a_	7	c2g19 A_
8	c2p0u B_	8	c3uep B_	8	c3oul A_
9	c3ov3 A_	9	d1o6a a_	9	c3dkq B_
10	c1xet D_	10	c1zx6 A_	10	c3bvc A_
11	c1ee0 A_	11	c2eyx A_	11	d2iuw a1
12	d1u0u a1	12	c2bz8 B_	12	c2iuw A_
13	c3a5q A_	13	c1z9q A_	13	c3gjb A_
14	d1u0v a1	14	c2e63 A_	14	c3itq B_
15	c1u0m A_	15	d1i07 a_	15	c3btz A_
16	c2h84 A_	16	c4glm D_	16	c2dbi A_
17	c3e1h A_	17	c2dbk A_	17	d2csg a1
18	c3euo B_	18	c2nwm A_	18	c2ijj A_
19	d1ee0 a1	19	d1uue a_	19	d2fdi a1
20	d1u0m a1	20	c2d1xD	20	c2opw A_

Table 4: Aligned regions for F-3,5-H, DFR and FLS. . The tables below show the domains used to establish the enzyme model by aligning the top 20 best hits that match highly with the target sequence. The confidence key in table 6 is used to show the probability with which the target sequence matches the available structures

Aligned regions in F-3,5-H		Aligned regions in DFR		Aligned regions in FLS	
1	c3ebs A_	1	c2iod D_	1	d1gp6 a_
2	d1nr6 a_	2	c1z7e C_	2	d1lodm a_
3	d2nnj a1	3	c1z45 A_	3	c3oox A_
4	c3e4e A_	4	d1i24 a_	4	d1w9y a1
5	d3czh a1	5	c2p4h X_	5	d1dcs a_
6	d1po5 a_	6	c2rh8 A_	6	c3on7 C_
7	d1r9o a_	7	d2c5a a1	7	c3oui A_
8	d2ij2 a1	8	d1y1p a1	8	c2g19 A_
9	c2iag A_	9	c2v6g A_	9	c3dkq B_
10	c2hi4 A_	10	d1oc2 a_	10	d2iuw a1
11	d1tgn a_	11	c2b69 A_	11	c2iuw A_
12	c2x2n B_	12	d2b69 a1	12	c3btz A_
13	c3na0 B_	13	c2x4g A_	13	c3itq B_
14	c3k9v B_	14	c2hun B_	14	c3bvc A_
15	c3g1g C_	15	c4egb C_	15	c3pvj B_
16	d2cib a1	16	d2bll a1	16	c2dbi A_
17	c3hf2 A_	17	d1r6d a_	17	d1otj a_
18	c3egm A_	18	d1kew a_	18	d2fdi a1
19	c2f9g A_	19	d1e6u a_	19	c2opw A_
20	c3juv A_	20	c3enk B_	20	c3tht B_

Table 5: Aligned regions in ANS, ANR and ANR2. . The tables below show the domains used to establish the enzyme model by aligning the top 20 best hits that match highly with the target sequence. The confidence key in table 6 is used to show the probability with which the target sequence matches the available structures

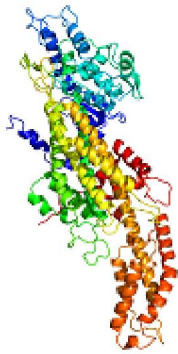
Aligned region in ANS		Aligned region in ANR		Aligned region in BPR	
1	d1gp6a	1	c1z45A	1	c3ptkB
2	d1odma	2	c1z7eC	2	c2rgmA
3	d1w9ya1	3	c2rh8A	3	c2dgaA
4	c3ooxA	4	d1i24a	4	d1cbga
5	d1dcsa	5	c2iodD	5	c3gnoA
6	c3on7C	6	c2p4hX	6	c3u57A
7	c2g19A	7	d2c5aa1	7	d1v08a
8	c3dkqB	8	c2v6gA	8	c4a3yA
9	c3ouiA	9	d1oc2a	9	d1e4mm
10	c3btzA	10	d2b69a1	10	d1v02a
11	d2iuwa1	11	c2b69A	11	c1v02F
12	c2iuwA	12	c1n7gB	12	c2if7B
13	c3thtB	13	c3enkB	13	d1qoxa
14	c3itqB	14	d1r6da	14	d2i78a1
15	c2dbiA	15	d1y1pa1	15	c3fiyA
16	c3bvcA	16	d1kewa	16	c3ahyD
17	d2csga1	17	c2hunB	17	c3ahxC
18	d2fdia1	18	c2p5uC	18	c4b3kA
19	c2ijjA	19	d1n7ha	19	d1gnxa
20	c3ms5A	20	d1e6ua	20	c3ai0A

Table 6: Aligned regions in BPR, PSY and the confidence key for alignment. . The tables below show the domains used to establish the enzyme model by aligning the top 20 best hits that match highly with the target sequence. The confidence key in table 6 is used to show the probability with which the target sequence matches the available structures

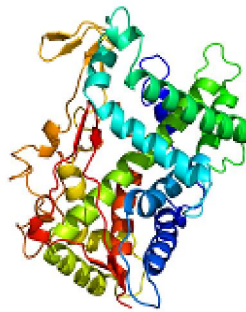
Aligned region in LAR		Aligned region in PSY		Confidence Key
1	c1z7eC	1	c2zcpA	 <p>High (9) Low (0)</p>
2	c1z45A	2	c4hd1A	
3	c2rh8A	3	d1e7fa	
4	d1j24a	4	c1wy0A	
5	c2iodD	5	c3mzvB	
6	c2p4hX	6	c3aq0G	
7	d1oc2a	7	c3oacD	
8	c2b69A	8	c3aqbD	
9	d2b69a1	9	c3oyrB	
10	c2v6gA	10	c3ts7B	
11	c1n7gB	11	c3n3dB	
12	c3enkB	12	c3nf2A	
13	d2c5aa1	13	c3m9uD	
14	d1y1pa1	14	c3lk5A	
15	d1rpna	15	c4dhdA	
16	d1n7ha	16	c1wmw	
17	c2p5uC	17	d2n80a1	
18	c3lu1C	18	c3lmdA	
19	c2z1mC	19	c2e8xB	
20	c2hrzA	20	c2azjB	

3.3 Protein Models

All enzyme models in Figure 1 except PSY Figure 1 (o) are modeled using the automated PHYRE approach giving models that had 70% and above coverage. These are good quality models.



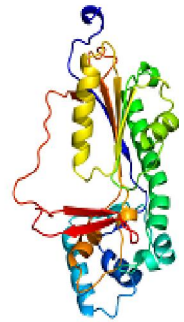
(a) PAL



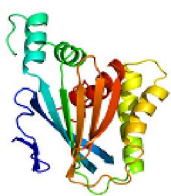
(b) C4H



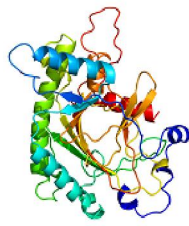
(c) 4CL



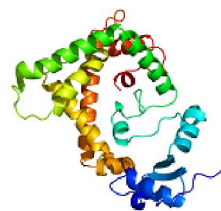
(d) CHS



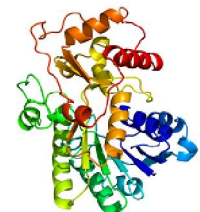
(e) CHI



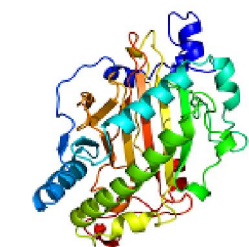
(f) F3H



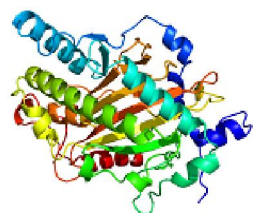
(g) F-3,5-H



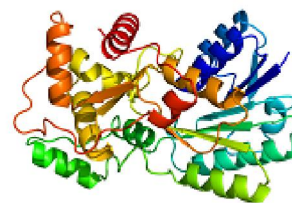
(h) DFR



(i) FLS

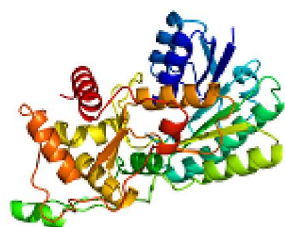
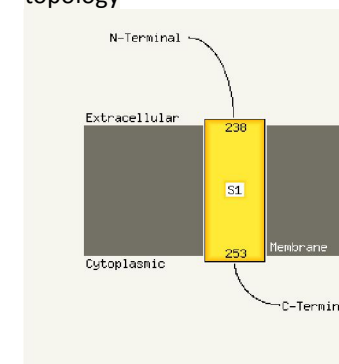


(j) ANS

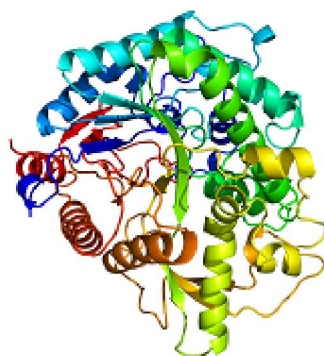


(k) ANR

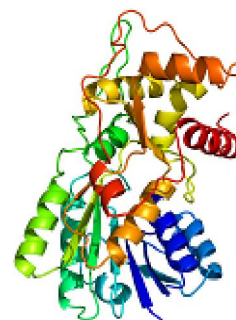
Transmembrane helices were predicted in sequence for ANR to adopt the topology



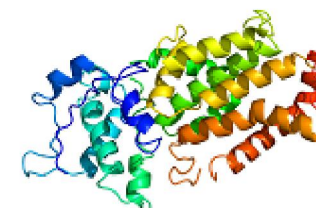
(l) ANR2



(m) BPR



(n) LAR



(o) PSY

Figure 1: Summary of all enzymes as predicted by phyre2 server

(a) PAL, (b) C4H, (c) 4CL, (d) CHS, (e) CHI, (f) F3H, (g) F35H, (h) DFR, (i) FLS, (j) ANS, (k) ANR, (l) ANR2, (m) BPR, (n) LAR, (o) PSY

The 3DLigandSite server was used for protein binding site prediction. Confident models produced by Phyre2 (confidence >90%) were automatically submitted to 3DLigandSite. This happened for all enzymes except PSY that was modeled through de novo approach and thus was submitted manually.

3.4 Cavities Identified In CASTP Server

Pockets are empty concavities on a protein surface into which solvent can gain access. Binding sites and active sites of proteins and DNAs are often associated with structural pockets and cavities. It provides identification and measurements of surface accessible pockets as well as interior inaccessible cavities, for proteins and other molecules. It measures analytically the area and volume of each pocket and cavity, both in solvent accessible (SA) surface and molecular surface (MS). The calculation uses a solvent probe of radius 1.4 angstrom.

Table 5: Summary of the five biggest pockets in each enzyme, their areas and the volume they occupy

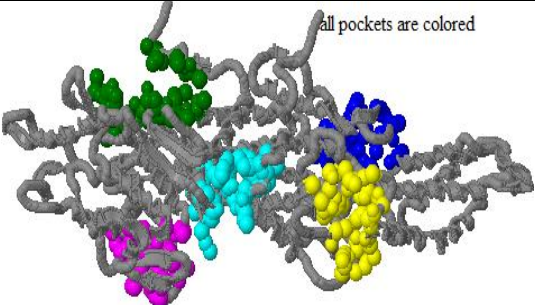
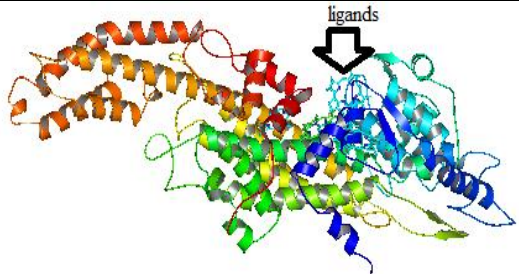
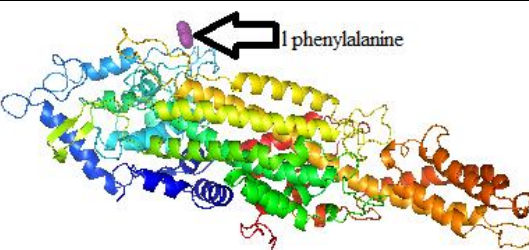
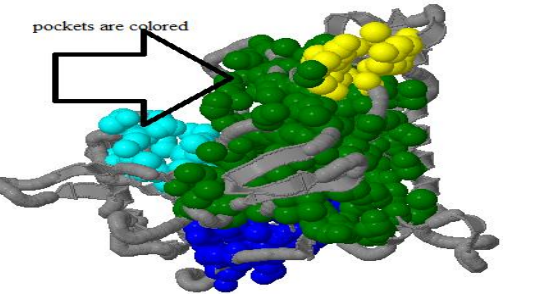
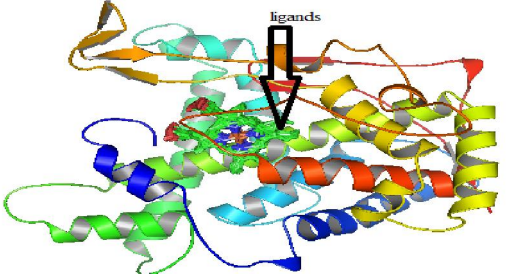
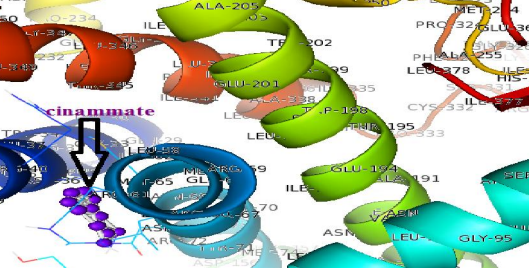
Enzyme	Area	Volume	Enzyme	Area	Volume
PAL	438.3	1289.8	FLS	1703.5	2611.1
	520.3	677		693.6	1160.7
	482.5	626		236.5	214.1
	398.7	649.5		234.5	238.9
	387.4	393.3		141.8	123.1
CH4	3206.4	4447.3	ANS	2184.2	3904.9
	956.1	907.5		286.6	301.1
	373.4	417.7		149.3	122.9
	317.6	309.5		65.9	48.3
	236	236.2		118	91.6
4CL	2015.2	2752.7	ANR	952.3	1731.4
	496.1	1119.3		399	579.9
	261.9	490.1		452	600
	226.2	349.7		284.1	344.8
	259.6	269		171.9	174.8
CHS	394.5	734.7	ANR2	1431.8	1940
	148.7	133.1		634.5	976.5
	139.9	133.5		206.8	183.7
	109	128.8		145.8	196.6
	159.9	133.4		121.6	153.2
CHI	1001.5	1283.1	BPR	498.2	885.5
	600.9	938		287.7	293.6
	83.1	68.9		302.7	304.9
	95	70.1		172.6	178.6
	116	136.9		165.6	164.5
F3H	2605.8	4337.1	LAR	1033.9	1390.4
	366.4	398.1		303.8	368.1
	304.9	452		160.8	386.2
	183.4	179.4		121.6	153.2
	119.4	150.3		122.8	144.7
F35H	1737.1	3069.2	PSY	3490.1	4851
	208.3	431.7		1457.5	2959.7
	218.7	185.2		281.3	293.1
	213.1	215.5		213.7	163.8
	134.5	217		162	107.1
DFR	1616.3	2807.7			
	146.2	408.4			
	91.6	106.8			
	66.5	60.7			
	117.5	84.6			

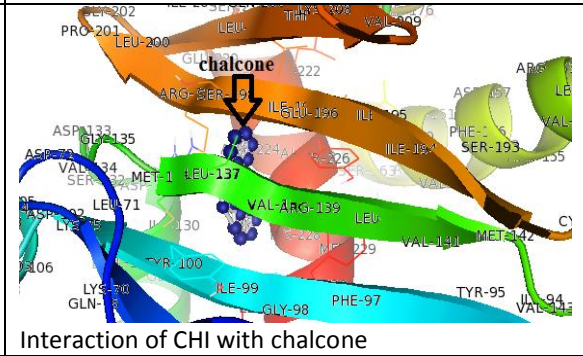
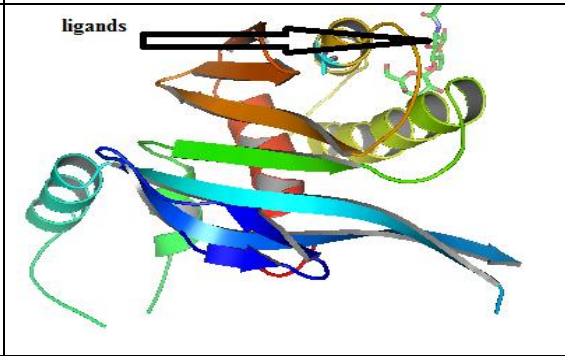
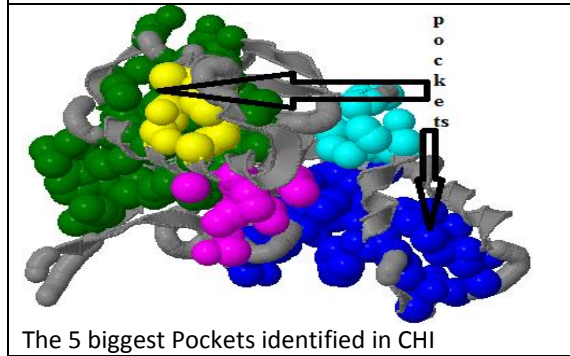
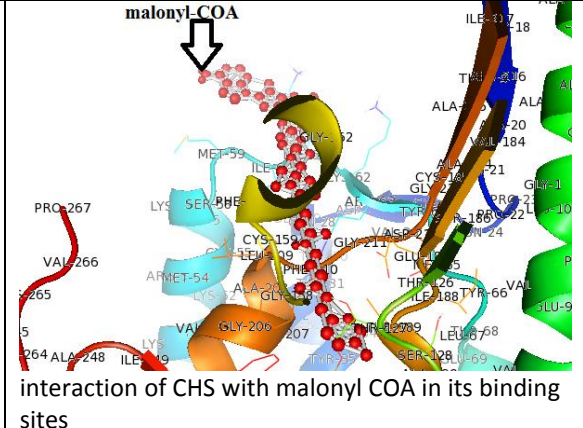
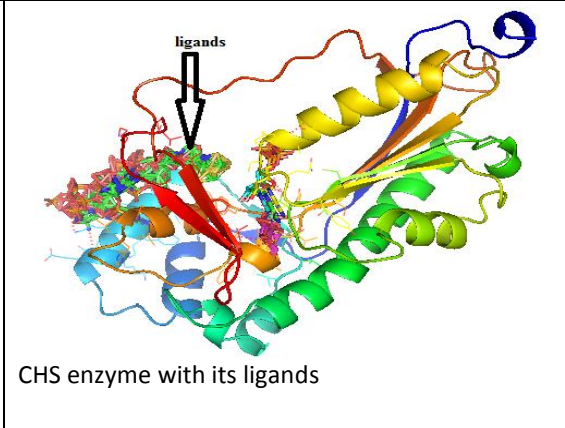
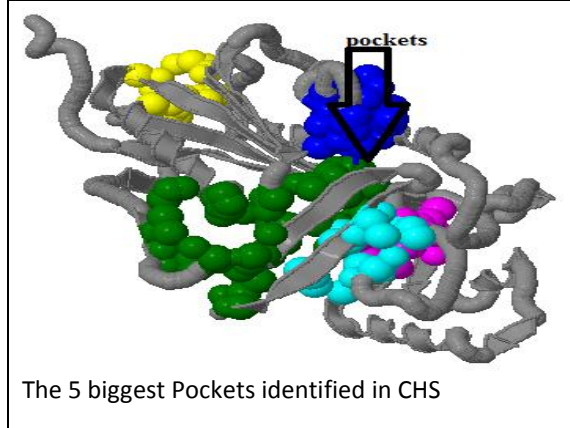
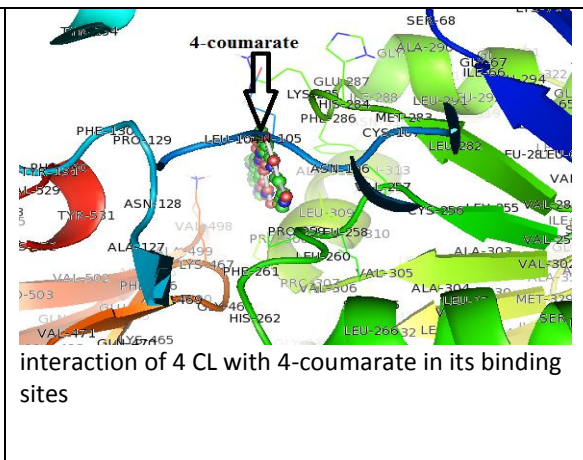
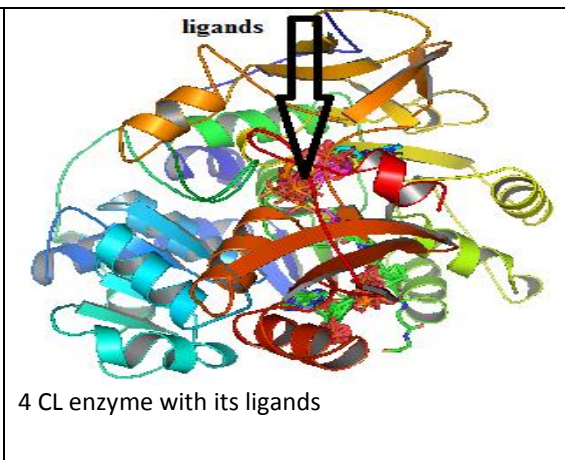
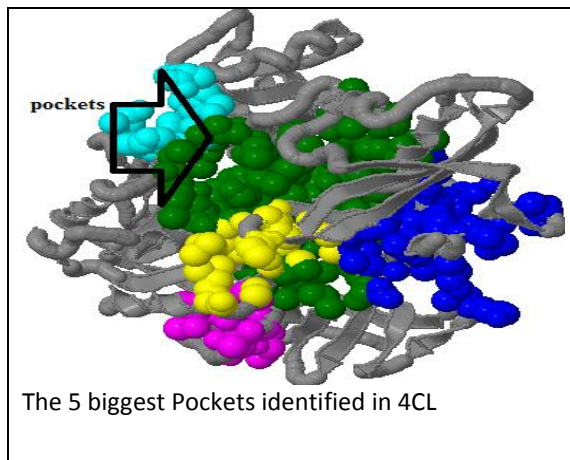
3.5 Enzyme Models, Pockets and Interactions with Substrate and Cofactors

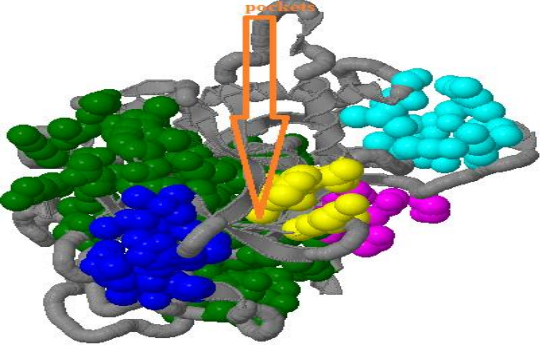
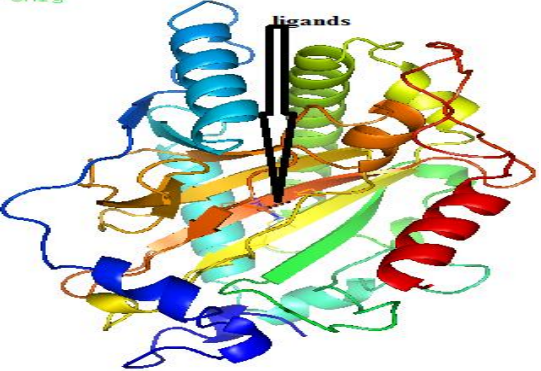
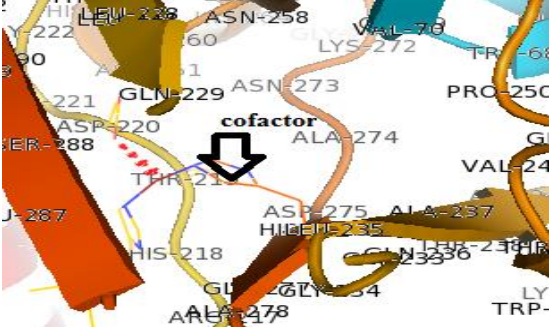
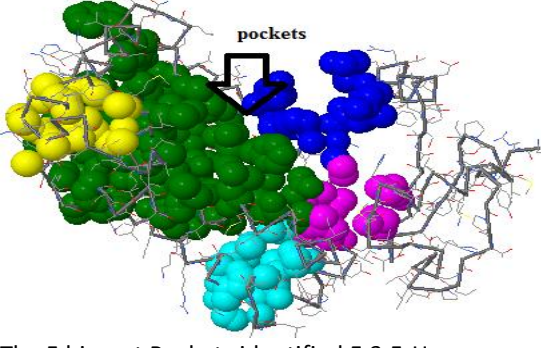
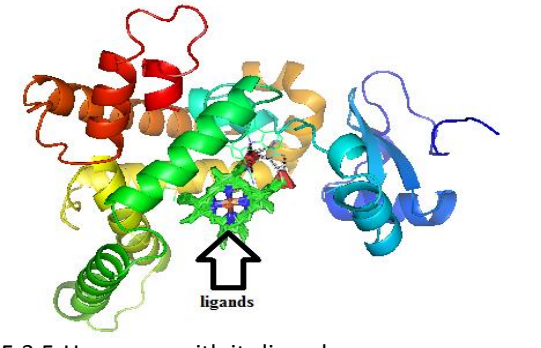
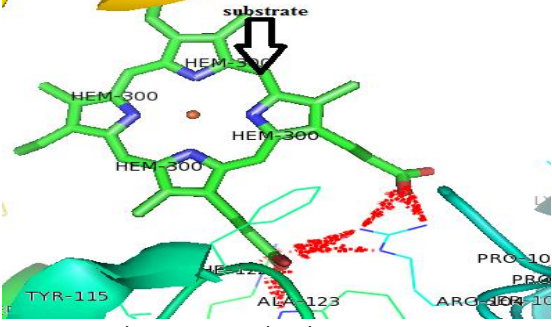
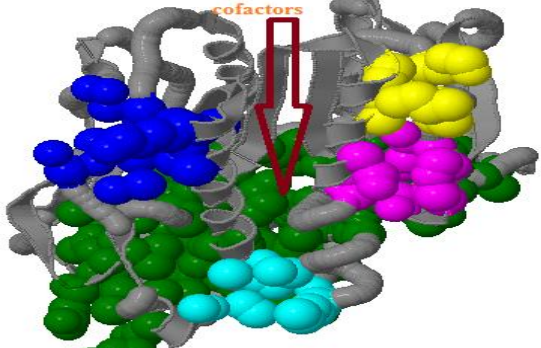
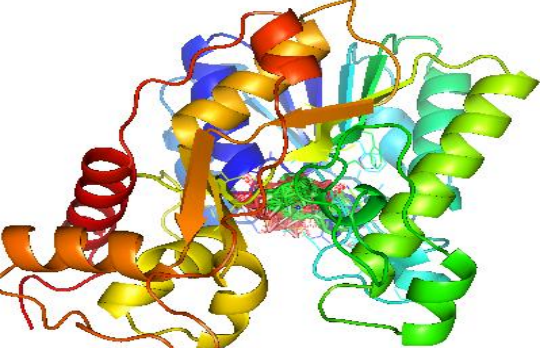
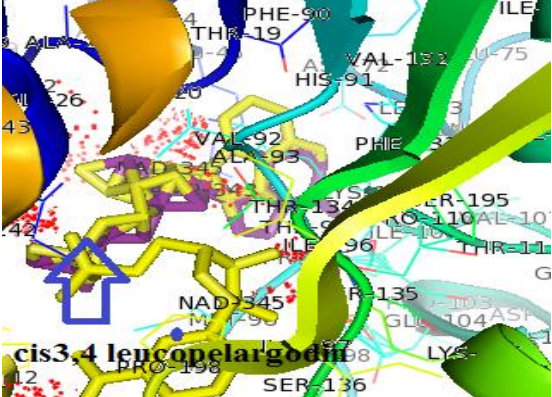
Docking is a method that produces the preferred orientation of one molecule to the second when both are bound together forming a complex. The association between biologically relevant molecules in this case enzymes and their substrates or enzymes and their cofactors play a key role in catalytic reaction. The enzymes are the hosts / receptors that receive the molecule. Ligands are the complimentary molecules which get bound to the receptors. They are the substrates and cofactors that act on each enzyme in the catalytic reactions to release products.

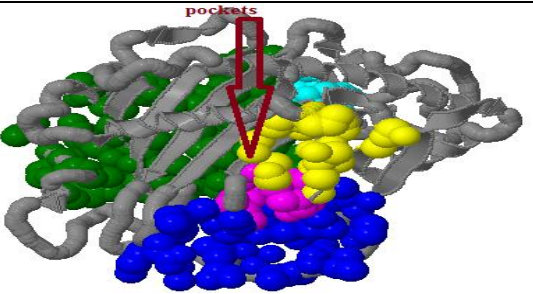
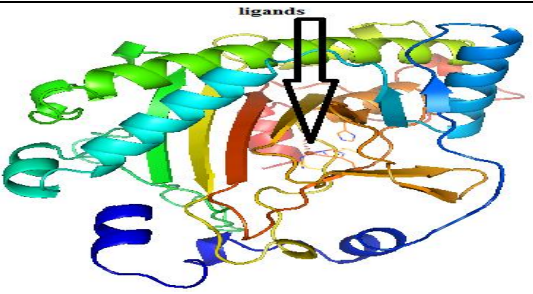
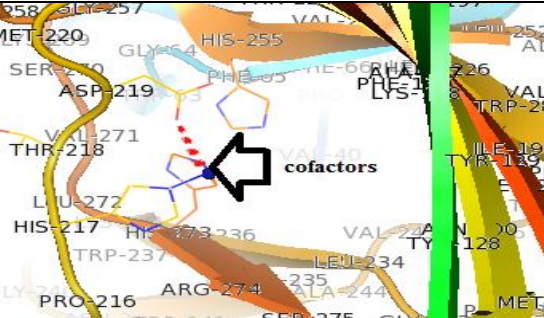
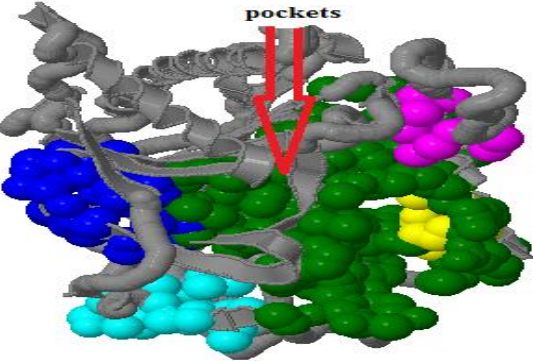
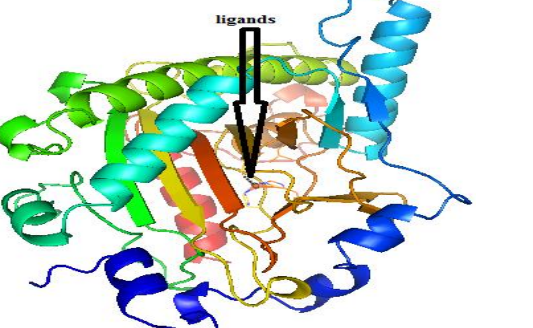
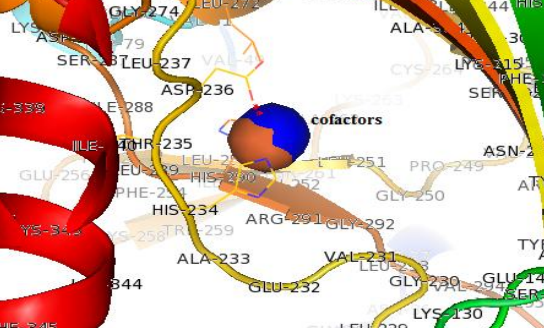
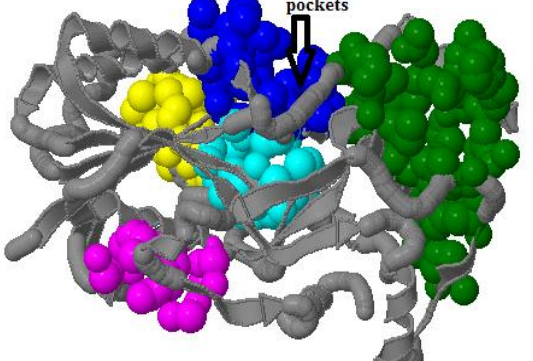
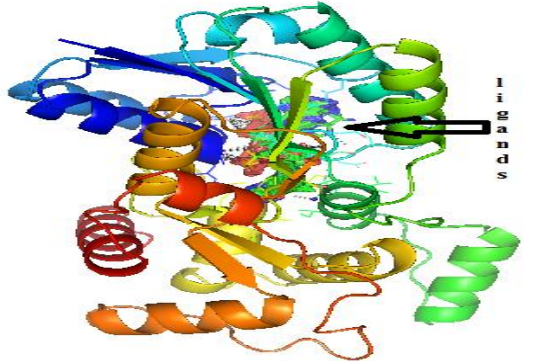
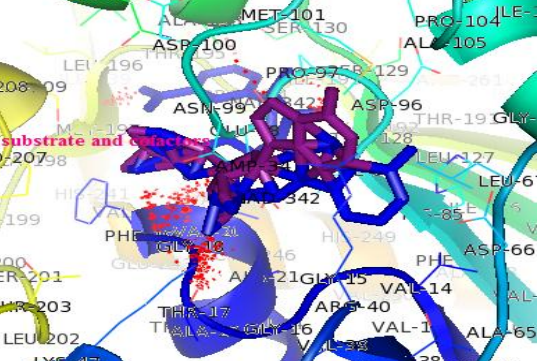
Column one indicates the pockets identified in each of the modeled structure of the enzymes, column two displays the ligands that bind to these pockets and column three shows the specific interaction of the enzyme with its substrates/ cofactors. Docking indicated results of computational simulation of interaction between the enzymes and their substrate and cofactors in their binding sites and the contact residues that the ligands attached to.

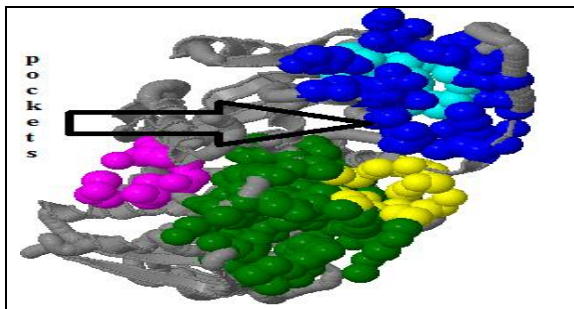
Table 6: enzyme structures with their ligands in their predicted cavities and the interactions

 <p>The 5 biggest Pockets identified in PAL</p>	 <p>PAL superimposed with its ligands</p>	 <p>Interaction of PAL with I phenylalanine in its binding sites</p>
 <p>The 5 biggest Pockets identified in C4H</p>	 <p>C4H superimposed with its ligands</p>	 <p>Interaction of C4H cinammate in its binding sites</p>

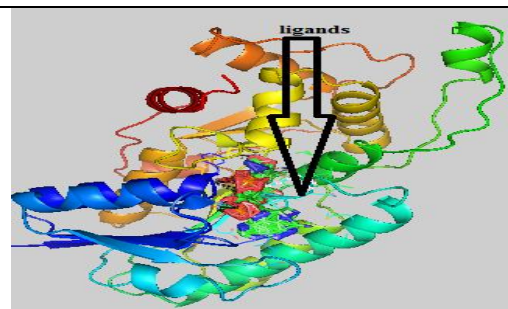


 <p>The 5 biggest Pockets identified in F3H</p>	 <p>F3H with its ligands</p>	 <p>F3H cofactors in its binding sites</p>
 <p>The 5 biggest Pockets identified F-3,5-H</p>	 <p>F-3,5-H enzyme with its ligands</p>	 <p>F-3, 5-H substrate in its binding site</p>
 <p>The 5 biggest Pockets identified in DFR</p>	 <p>DFR enzyme with its ligands</p>	 <p><i>cis</i>-3,4 leucopelargonin</p>

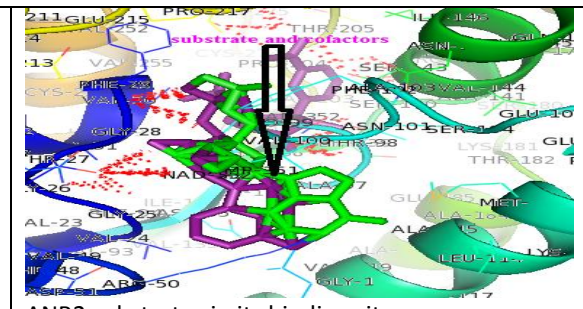
 <p>The 5 biggest Pockets identified in FLS</p>	 <p>FLS enzyme with its ligands</p>	 <p>DFR with its substrate in its binding sites</p> <p>FLS with its cofactors in its binding sites</p>
 <p>The 5 biggest Pockets identified in ANS</p>	 <p>ANS enzyme with its ligands</p>	 <p>ANS with its cofactors in the binding sites</p>
 <p>The 5 biggest Pockets identified in ANR</p>	 <p>ANR enzyme with its ligands</p>	 <p>ANR substrates in the binding sites</p>



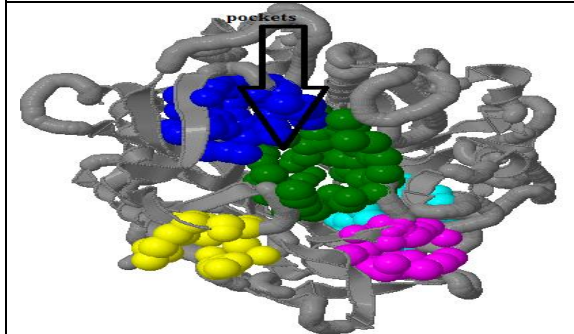
The 5 biggest Pockets identified in ANR2



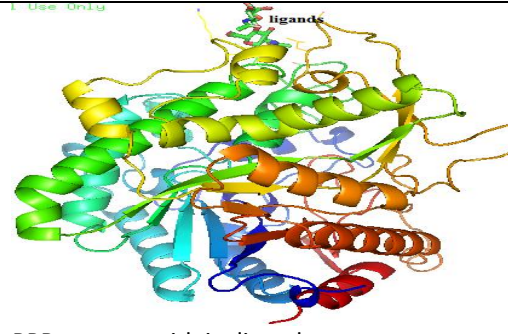
ANR2 enzyme with its ligands



ANR2 substrates in its binding sites



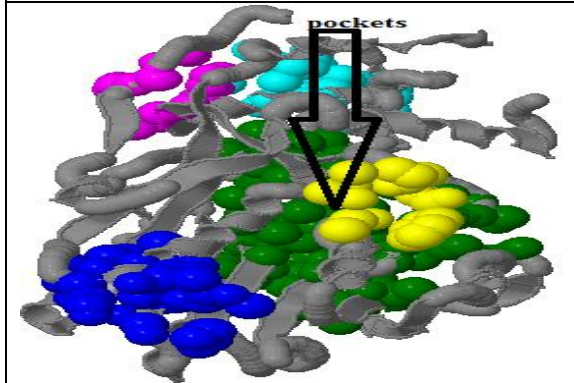
The 5 biggest Pockets identified in BPR



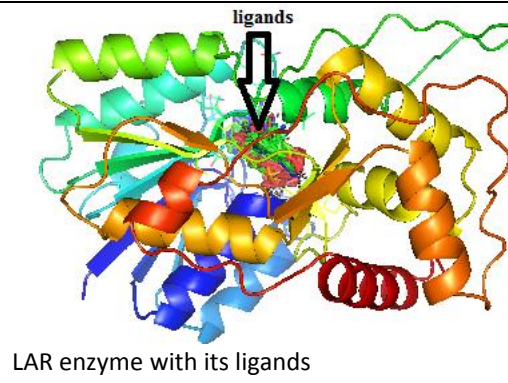
BPR enzyme with its ligands



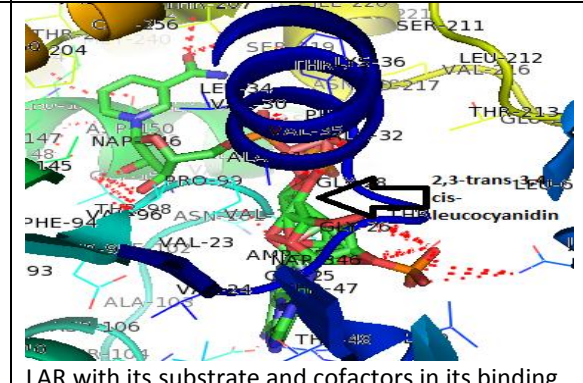
BPR with its cofactors in the binding sites



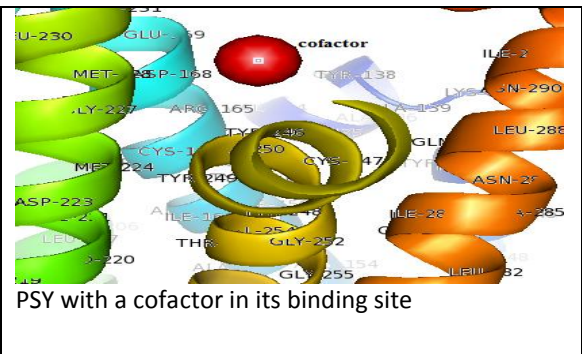
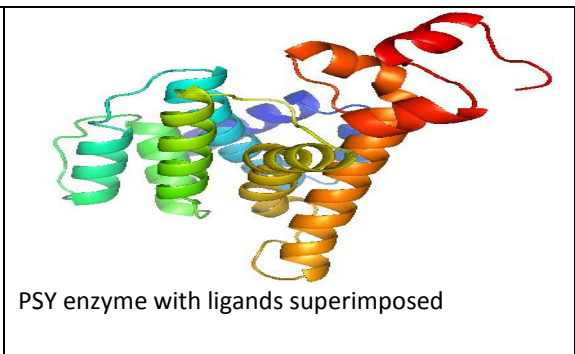
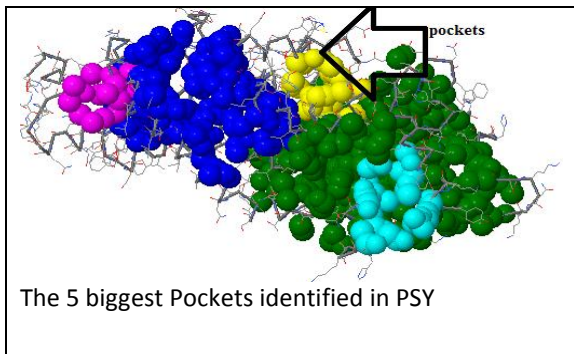
The 5 biggest Pockets identified in LAR



LAR enzyme with its ligands



LAR with its substrate and cofactors in its binding site.



4.0 Conclusion

Tea is a popular beverage as a source of beneficial secondary metabolites. The bestselling tea is believed to be high quality tea owing to synthesized secondary metabolites. Tea however requires long conventional breeding time thus; it is not really advisable to improve crop varieties. From this study it is clear that the secondary metabolites in tea are synthesized as a result of action of some enzymes. The modeled three-dimensional structures of these enzymes are related to their functions. The modeled structure aided in the identification of the putative substrate binding sites which indicates that there is an interaction between enzyme-substrate and enzyme-cofactor. Docking simulated a candidate ligand binding into the receptor indicating that the substrates and cofactors bind into the active sites of the ligand. This interaction leads to catalytic action resulting onto various products of the biosynthetic pathways. This study provides a valuable insight into the mechanism of action of enzymes aiding in the ultimate aim of improving tea quality and enhance the beneficial health properties. It therefore forms a basis of improving the quality of tea computationally rather than using the long conventional breeding approach.

Acknowledgements

Research assistants in Jomo Kenyatta University of Agriculture and Technology department of Biochemistry

References

- Kelley, L. A. and Sternberg, M. J. E. (2009). *Nature Protocols*, **4**: pp 363 - 371 [pdf] [Import into BibTeX]
- Liang, J., Edelsbrunner, H., Fu, P., Sudhakar, P. V. and Subramaniam, S. (1998b). Analytical shape computation of macromolecules. II. Identification and computation of inaccessible cavities in proteins.
- Larkin, M. A., Blackshields, G., Brown, N. P., Chenna, R., McGettigan, P. A., McWilliam, H., Valentin, F., Wallace, I. M., Wilm, A., Lopez, R., Thompson, J. D., Gibson, T. J. and Higgins, D. G. (2007). Clustal. W. and Clustal, X. version 2.0. *Bioinformatics*, **23** (21): ppp 2947-2948.
- Proteins: Struct. Funct. Genet.* **33**:18-29.
- Liang,(2006). CASTp: computed atlas of surface topography of proteins with structural and topographical mapping of functionally annotated residues. *Nucl. Acids Res.*, **34**:ppW116-W118.
- Luczaj, W., Skrzydlewska, E. (2005). Antioxidative properties of black tea. *American Journal of Preventive Medicine*. **40**(6):pp910-918.
- Park, J. S., Kim, J. B., Hahn, B. S., Kim, K. H., Ha, S. H., Kim, Y. H. (2004). EST analysis of genes involved in secondary metabolism in *Camellia sinensis* (tea), using suppression subtractive hybridization.
- Rawat, R. and Gulati, A. (2008). Seasonal and clonal variations in some major glycosidic bound volatiles in Kangra tea (*Camellia sinensis* (L.) O. Kuntze). *Journal European Food Research and Technology*, **226**(6):pp 1241-1249.
- Tanaka, J., Taniguchi, F. (2006). Estimation of the genome size of tea (*Camellia sinensis*), *camellia* (*C. japonica*), and their interspecific hybrids by flow cytometry. *Journal of the Remote Sensing Society of Japan*, **101**: pp 1–7.
- Wang, Y., Jiang, C. J., Zhang, H. Y. (2008). Observation on the Self-incompatibility of Pollen Tubes in Self-pollination of Tea Plant in Style *in vivo*. **28**:pp429–435.
- Wang, X. W., Luan, J. B., Li, J. M., Bao, Y. Y., Zhang, C. X. and Liu, S. S. (2010). *De novo* characterization of a whitefly transcriptome and analysis its gene expression during development. *BMC Genomics*, **11**: pp 400.
- Wass, M. N., Kelley, L. A. and Sternberg, M. J. (2010). *Nucleic Acids Research* **38**, W469-73 [pubmed]